




# Event-based and continuous flood modeling in Zijinguan watershed, Northern China

Rajeev Katwal<sup>1,2</sup> · Jianzhu Li<sup>1,2</sup> · Ting Zhang<sup>1,2</sup>  · Chunqi Hu<sup>1,2</sup> · Muhammad Akbar Rafique<sup>1,2</sup> · Yanchen Zheng<sup>1,2</sup>

Received: 24 November 2020 / Accepted: 16 March 2021 / Published online: 8 April 2021  
© The Author(s), under exclusive licence to Springer Nature B.V. 2021

## Abstract

Hydrological models are a conceptual representation of a simplified hydrological cycle. The hydrological cycle is the water cycle that circulates water from the land surface to the atmosphere and back again to the land. With the use of Hydrologic Engineering Center-Hydrologic Modeling System (HEC-HMS), an event-based model and a continuous hydrological model were established in Zijinguan watershed of Daqinghe River basin. To study the loss methods provided by HEC-HMS and its appropriateness for model fitting, is the main objective of this paper. The watershed was delineated with HEC-GeoHMS in ArcGIS, and its properties were extracted from a Digital Elevation Model (DEM) of 30 m × 30 m. The HEC-HMS includes a soil conservation service curve number (SCS-CN) method and a soil moisture calculation (SMA) loss method, simulating the event and continuous runoff, respectively. SCS Unit hydrograph and Muskingum were used for flow routing. Specifically, eight rainfall events were selected for calibrating (6 events) and verifying (2 events) the event-based model. Similarly, for the continuous model the wet seasons of eight different years were used for calibration and verification. The calibrated parameters of the events model were used in the continuous model. The soil moisture and evapotranspiration data were decoded from the satellite data to set in the continuous model. The performance of SCS-CN and SMA models was compared. During the calibration period, the values of NSE, PEV and PEPF range from 0.605 to 0.744, 3.1 to 13.58%, and 11.104 to 27.72%, and during validation they are 0.527 to 0.634, 4.35% to 5.01%, and 13.66% to 27.88%, for SCS-CN model. For the SMA model, the values of NSE, PEV and PEPF during calibration range from 0.434 to 0.604, 2.879 to 34.326%, -4.831 to 57.48%, and during validation they are 0.094 to 0.624, -19.52% to -12.55%, and 40.213% to 50.15%. Overall, the performance of SCS-CN model is found more satisfactory than that of SMA model.

**Keywords** HEC-HMS · SCS-CN · SMA · Satellite data · Calibration and validation · Model performance

---

✉ Ting Zhang  
zhangting\_hydro@tju.edu.cn

<sup>1</sup> State Key Laboratory of Hydraulic Engineering, Simulation and Safety, Tianjin University, Tianjin, People's Republic of China

<sup>2</sup> Hydrological and Water Resources, Survey Bureau of Hebei Province, Shijiazhuang 050031, People's Republic of China

## 1 Introduction

Hydrology is of great importance to humans and the environment, which applies to all phases of the earth's water (Chow et al. 1988). Hydrological modeling helps to understand all the rainfall-runoff processes (Ouedraogo et al. 2018) and is a simplified representation of the real situation, which is a challenging task, especially for those areas that lack available data (Yu and Schwartz 1998). Therefore, the hydrological model is a key and significant tool in water resources engineering and used for different purposes: streamflow predicting, flood inundation mapping, structure design, and water resources planning, and so on (McCuen 1998; Davie 2002). On the basis of conceptual representation of the water flow process, many hydrological models have been proposed to simulate the rainfall-runoff process throughout the basin (Madsen 2000; Yener and Orman 2008; Li et al. 2008; Stisen and Jensen 2008). Jajarmizadeh et al. (2012) show the dominant classifications for hydrological models alongside the different views from past to present.

Physical models and Abstract (mathematical) models are two main categories of hydrological model (Chow et al. 1988). Further, hydrological models can be divided into two subcategories: stochastic and deterministic. Deterministic models do not provide randomness, but on the other hand, stochastic models produce outputs that are partially random (Tassew et al. 2019; Kaczmarek 1976; Jajarmizadeh et al. 2012). Cunderlik (2003) further classified deterministic hydrologic models into three major categories:

1. the lumped model, which assesses the catchment response simply at the outlet without obviously counting for individual sub-basins responses
2. the semi-distributed model, which is partly allowed to change in space with the separation of catchments into an amount of sub-basins
3. the distributed model, which allows parameters changing in space. Semi-distributed models are more physically based than lumped models, and they require less input parameters in comparison with distributed models (Jajarmizadeh et al. 2012).

Hydrological models such as Hydrological Simulation Program-Fortran (HSPF), MIKE-SHE, Topography Based Hydrological Model (TOPMODEL), Soil and Water Assessment Tool (SWAT, Davis et al. 2004), Hydrological Engineering Center Hydrological Modeling System (HEC-HMS), and Modular Modeling System (MMS), were proposed in the literature to estimate the runoff on the basis of available data and complexity of its own system. Among these models, the Hydrologic Modelling System (HEC-HMS), a modeling software which was developed by the US Army Corps of Engineers Hydrologic Engineering Center in 1998, was used in this study for flood modeling. This semi-distributed model can be used for flood simulation with hourly data (Abushandi and Merkel 2013). Parameter-based modeling and distributed parameter-based modeling are supported in this HEC-HMS model (Agrawal 2005). Event-based and continuous modeling can be done in HEC-HMS (Arekhi 2012).

Several researches have been done in HEC-HMS to prove its capability to simulate the streamflow. Samarasinghea et al. (2010) applied HMS to predict runoff for 50 years' rainfall in Kalu-Ganga river of Sri Lanka. Oleyiblo and Li (2010) applied HMS to simulate peak discharge for the purpose of flood forecasting in Misai and Wan'an catchments in China. They obtained acceptable simulation results. Meenu et al. (2013) used HEC-HMS 3.4 to estimate the impacts of possible future weather change situations on the hydrology of the Tunga-Bhadra River, upstream of the Tungabhadra dam. Bhuiyan et al. (2017) predicts

the flood in Sturgeon Creek watershed in Canada using satellite derived soil moisture data with HEC-HMS. De Silva et al. (2014) applied HEC-HMS for a case study of event and continuous hydrologic modeling in the Kelani River basin in Sri Lanka and confirmed applicability of HEC-HMS in flood control, disaster mitigation and water management in medium-sized watershed. Azmat et al. (2016) have successfully applied HEC-HMS model for event- and continuous-based modeling in high-altitude catchment to reproduce the streamflow under potential changing climate situations.

Hydrological modeling can be event-based or continuous, depending on the application. Event-based models simulate individual flood events. Continuous models simulate long-term runoff series using soil type data and atmospheric data. For the event-based and continuous hydrological modeling, a large number of spatial and temporal data such as land use/land cover, topography, soil moisture, soil type, precipitation, observed discharge data are required. Actually, the accessibility and reliability of these data are often a problem to deal with. Sometimes it is necessary to compromise the overall quality of the simulation due to the lack of high-resolution data for model calibration and verification (Chu and Alan 2009). Todini (1996) stated that the accuracy of the results is often influenced by data quality than the quality of the model. In recent researches the rate of using soil moisture estimated from satellite data for hydrologic modeling has been increased, since measured data are rare (Brocca et al. 2010; Sutanudjaja et al. 2013). Several studies were carried out to define the applicability of satellite data in flood modeling. Trambly et al. (2012) stated that satellite data products were capable of reproducing relatively accurate daily dynamics of soil moisture at the catchment scale. Li et al. (2016) presented current improvements in integrating satellite soil moisture data and a rainfall-runoff model to predict rain-induced floods.

The current study presents event-based and continuous hydrological modeling of Zijingguan Watershed. The main objectives are to: (1) establish HEC-HMS model for flood simulation based on remote sensing soil moisture and evapotranspiration data in Zijingguan watershed; (2) make comparison of SCS-CN-based and SMA-based model performance to test the applicability of the event-based and continuous modeling in HEC-HMS.

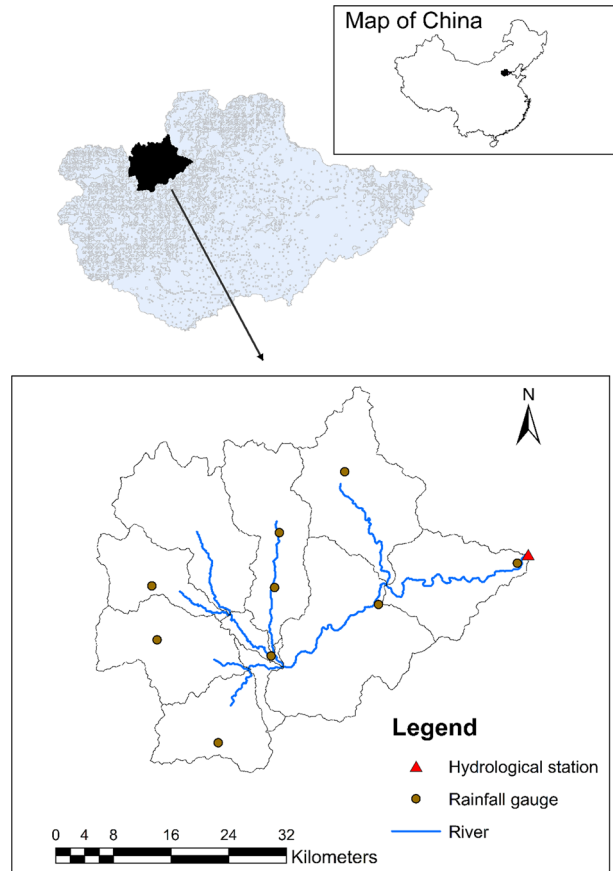
## 2 Study area

The Daqinghe River Basin is located in the northeastern portion of China ( $113^{\circ} 39' - 116^{\circ} 10' E$ ,  $38^{\circ} 23' - 40^{\circ} 09' N$ ), with the municipality of Beijing in the north and the municipality of Tianjin in the east. (Fig. 1). The basin has a total area of 43,065 km<sup>2</sup> and includes Hebei Province, a small part of Shanxi Province and parts of the municipalities of Beijing and Tianjin (Li et al. 2019).

The basin area can be divided from west to east into three major geographical areas: mountainous region, transition zone, and plains area. The hilly terrain ranges from 100 to 2600 m of elevation and covers 40% of the basin area, with an uneven landscape and deep valleys. Most of the rivers flowing towards the basin originate in this mountain range. The plain occupies 50% of the basin, which is at an altitude between 10 m and the sea level. The transition zone covers 10% of the basin, with a gentle to moderate slope, ranging from 10 to 100 m elevation.

The study area is a sub-watershed of the Daqinghe River basin which is located on the upper part of the Juma River controlled by the Zijingguan hydrologic station. The drainage area of Zijingguan hydrologic station is 1776 km<sup>2</sup> as shown in Fig. 1. The length of the

**Fig. 1** Daqinghe river basin and the study area Zijinguan watershed with Rainfall gauge and Hydrological station



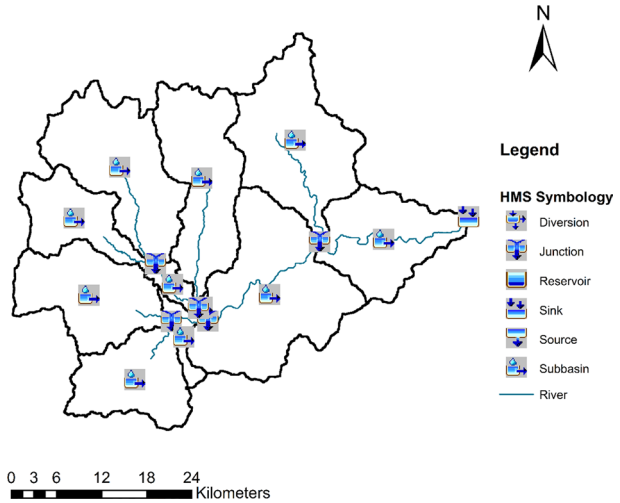
main-stream is 81.5 km with an average slope of 5.5%. It belongs to semi-arid and sub-humid climate zone, and the average annual precipitation recorded in this sub-watershed is about 650 mm. All the flood events observed in this hydrologic station are recorded in wet season (from June to September).

### 3 Data

#### 3.1 Terrain data

The Digital Elevation Model (DEM) data of the river basin are required in the HEC-GeoHMS (USACE-HEC-GeoHMS 2006) model. Digital elevation model (DEM) was acquired from Shuttle Radar Tropical Meteorology (SRTM) with a spatial resolution of 30 m (<http://www.gscloud.cn/>). Raw DEM was delineated in ArcGIS 10.1 using Arc Hydro tools, and basin model was developed using HEC-GeoHMS 10.2 (Baumbach et al. 2015). The watershed was divided into ten sub-watersheds, five junctions, five reaches and one outlet as shown in Fig. 2.

**Fig. 2** The delineation of sub-watersheds, reaches and junctions in the watershed



### 3.2 Rainfall data

Hourly rainfall data from 1972 to 2002 at eight rain gauges located in the Zijingguan watershed were obtained from Hydrology and Water Resource Survey Bureau of Hebei Province. This study period is chosen because rainfall data are only available up to 2002. For calibration and validation of event-based modeling, eight rainfall events were selected (Table 1). Similarly, eight wet periods which include the 8 flood events were taken for continuous modeling (Table 2).

### 3.3 Stream flow data

Discharge data at Zijingguan hydrologic station used in this research were obtained from Hydrology and Water Resource Survey Bureau of Hebei Province. The hourly data covering from 1972 to 2001 of wet seasons were collected for simulation.

**Table 1** The 8 rainfall events for flood events modeling

Flood event	Time period	Rainfall depth (mm)
13 August–15 August, 1973	3 days	45.7
17 July–22 July, 1976	4 days	106.8
24 Jun–01 July, 1977	8 days	107.7
26 July–29 July, 1978	4 days	91.3
30 July–02 August, 1982	4 days	87.4
14 July–17 July, 1987	4 days	9.2
01 August–04 August, 1988	4 days	61.5
05 July–07 July, 1998	3 days	70.2

**Table 2** The 8 wet periods for continuous flood modeling

Wet period	Time period	Rainfall depth (mm)
25 Jun–15 August, 1973	60 days	480.7
29 Jun–06 August, 1976	48 days	288.3
02 Jun–18 September, 1977	109 days	506.3
08 Jun–07 September, 1978	92 days	594.0
16 Jun–11 August, 1982	57 days	373.0
05 Jun–28 August, 1987	85 days	410.4
13 July–13 August, 1988	32 days	352.5
30 Jun–06 August, 1998	60 days	291.0

### 3.4 LULC and soil data

Land use and land cover (LULC) maps of 2000 were obtained from Global Land Cover Map (GLC 30 m, <http://westdc.westgis.ac.cn/data/flaacad-9f42-474e-8aa4-d37f37d6482f>), as shown in Fig. 3a. Soil data for this research were obtained from Harmonized World Soil Database (HWSD). Soil map was 1:1,000,000 scale and provided by the Institute of Soil Science, Chinese Academy of Sciences, as shown in Fig. 3b.

### 3.5 Soil moisture and evapotranspiration estimates from satellite data

Soil moisture and Evapotranspiration data were downloaded from a new NASA internet tool called Giovanni (<https://giovanni.gsfc.nasa.gov>).

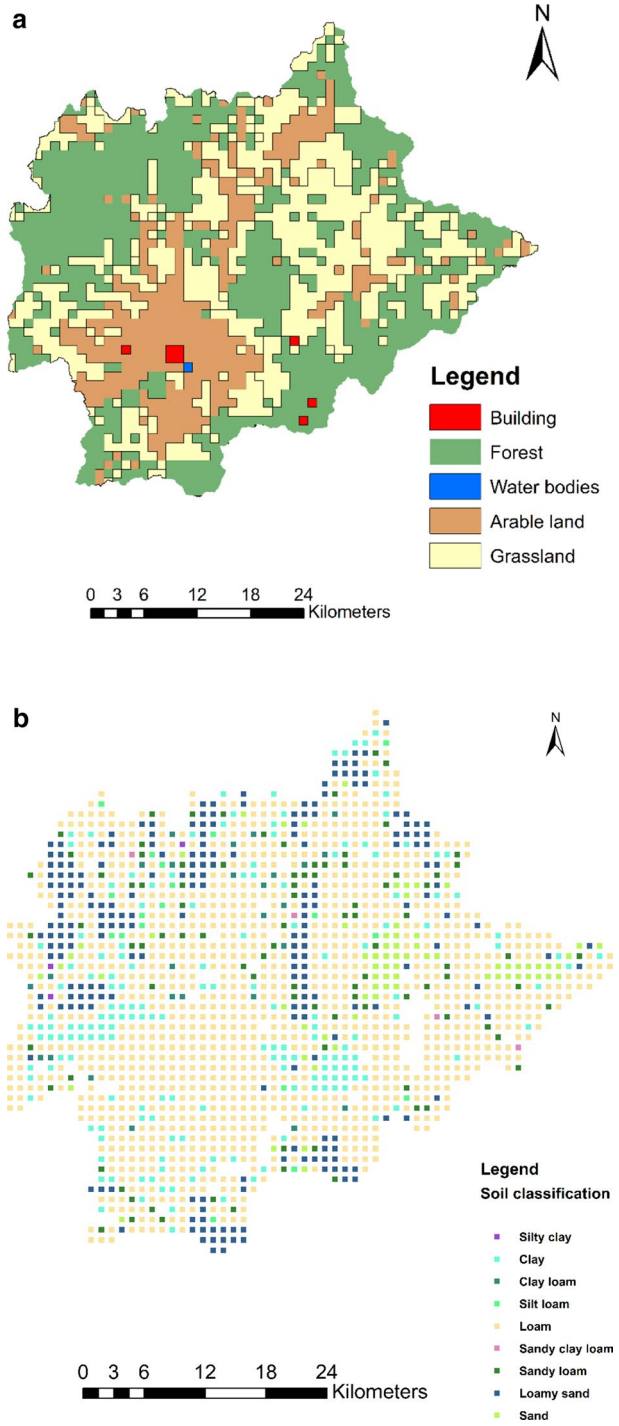
Hourly data of 1973, 1976, 1977, 1978, 1982, 1988, 1987 and 1998 are used in this study. For soil moisture and evapotranspiration, data of GLDAS model (global land data assimilation system) with spatial resolution of  $0.25^\circ$  are downloaded. Thiessen polygon method was used to estimate the average soil moisture of each sub-basin and similarly, for evapotranspiration too. The soil saturation required as initial condition in HEC-HMS is calculated as Eqs. (1) and (2):

$$S = \theta \times \phi^{-1} \times 100 \quad (1)$$

$$\phi = 1 - \frac{\rho_b}{\rho_s} \quad (2)$$

Volumetric water content is represented by  $\theta$ ,  $\rho_b$  is the bulk density, and  $\rho_s$  is specific density. Soil saturation percentage is denoted by  $S$ , and  $\phi$  is porosity. With Soil–Plant–Air–Water (SPAW) software, bulk density was calculated and specific density was taken from standard range ( $2.5 < \rho_s < 2.8$ ) g/cc. Soil moisture and evapotranspiration data were used in continuous SMA modeling.

**Fig. 3** Land use and soil data of the study area. **a** LULC cover; **b** Soil map



## 4 Methodology

### 4.1 HEC-HMS model description

HEC-HMS is a standard rainfall-runoff model which has been widely used for runoff simulation (Azmat et al. 2016). Among the nine different loss methods in HEC-HMS, some are for event-based simulation and some for continuous simulation. Seven different transformation methods, five recession methods and six routing methods are included in the model. The semi-distributed model can reflect the hydrological process at watershed scale (Bhuiyan et al. 2017). In current work, the Soil Conservation Service curve number loss method (SCS-CN, USDA 1986) was applied for event simulation, and Soil Moisture Accounting (SMA) loss method was applied for continuous simulation. SCS (Soil Conservation Service) unit hydrograph method was used to model the transformation of precipitation excess into direct runoff. Recession method was employed for baseflow, and Muskingum method was employed for channel routing.

#### 4.1.1 Modeling losses

**4.1.1.1 Soil Conservation Service Curve Number (SCS-CN)** This is the event-based rainfall-runoff model, which is one-parameter (CN) and empirical (SCS-CN, USDA 1986). The event-based simulations employed SCS-CN to estimate direct runoff from a specific or design rainfall (Hawkins et al. 2009). In current research, SCS-CN method is adopted primarily because it can be widely used in various environments and can completely utilize the spatially distributed GIS data available for the catchment, which are also processed with HEC-GeoHMS.

The SCS-CN model can be expressed as (USDA 1986):

$$R = \frac{P_e^2}{P_e + S} \quad (3)$$

where,

$$P_e = P - I_a \quad (4)$$

$$I_a = \alpha S \quad (5)$$

$$S = 2540 - \frac{25.4}{\text{CN}} \quad (6)$$

For a default value,  $\alpha=0.2$ . Cumulative runoff is represented by  $R$ , cumulative rainfall is denoted by  $P$ ; cumulative effective rainfall is represented by  $P_e$  ( $P_e > 0$ ; otherwise,  $R=0$ );  $S$  represents the potential maximum retention;  $I_a$  represents initial abstraction, which includes surface depression storage, vegetation interception, and infiltration; initial abstraction coefficient is  $\alpha$ , and CN is runoff curve number, which is a function of soil type, land cover and antecedent moisture condition (AMC). The CN value ranges from 100 (water bodies) to approximately 30 for permeable soils with high infiltration rates (Feldman 2000). Many researchers have used the geographic information system (GIS) to calculate the runoff curve number (Abouzar and Hamid 2014; Zhan and Huang



2004; Gandini and Usunoff 2004). Land use/Land cover is the important input parameter to the SCS-CN model (Pandey and Sahu 2007).

For each sub-basin unit, the curve number (CN) is calculated, followed by weighting of the area for the entire sub-watershed (Feldman 2000). The study area is in semi-arid climate, and it has AMC-II moisture content with an average condition:

$$CN = \frac{\sum cn_i a_i}{A} \quad (7)$$

where CN is weighted mean of curve number,  $cn_i$  is curve number in per unit,  $a_i$  is Area in per unit, and  $A$  is the total area of the basin.  $cn_i$  is estimated on the basis of hydrologic soil group, hydrologic condition and antecedent moisture condition (AMC).

**4.1.1.2 Soil Moisture Accounting (SMA)** The continuous simulation employed Soil Moisture Accounting (SMA). For modeling the movement of water through the soil surface and the deeper soil profile to the groundwater layers, SMA method is preferred (USACE-HEC 2000). This loss method uses five layers to represent the dynamics of water movement over and within the soil. The layers include canopy interception, surface depression storage, soil, upper groundwater, and lower groundwater. The values for the canopy and surface storage were obtained from the land use/land cover analysis, and soil geographic database map in ArcGIS and MS Excel as derived from values analysis from Holberg (2014) and Bennett (1998).

Initial value of initial canopy storage (%) and initial surface storage (%) is taken as 0% with respect to simulation period (Ahbari et al. 2018). Initial soil moisture condition is the soil saturation percentage derived from satellite estimated data, and GW 1% and GW 2% were estimated during the calibration process. The maximum infiltration rate has been specified as the upper limit of the rate of water entry from surface storage into the soil. And, the saturated hydraulic conductivity is represented to be the maximum infiltration rate and is obtained from Soil–Plant–Air–Water (SPAW). Soil storage was specified as the total storage of water available in the soil profile and tension storage is another component of the upper soil layer parameter. The calculation of soil storage and tension storage is done on basis of considering them by means of the porosity and soil field capacity based on the soil texture values (Ahbari et al. 2018). Impervious percentage area was evaluated using land use map. The average hydraulic conductivity of all sub-watersheds are obtained on the basis of soil texture from SPAW (Table 3), and these conductivity values are considered as the soil percolation rate and the first groundwater layer (GW1) percolation rate in the model (Singh and Jain 2015). GW1 and GW2 storage coefficient and storage depth were taken from standard ranges defined in Fleming and Neary (2004), and the final values were obtained during calibration process.

#### 4.1.2 Modeling direct runoff

For modeling the conversion of excess precipitation into direct surface runoff, the SCS Unit hydrograph method is used. The input is only the lag time ( $T_{lag}$ ). It is calculated for each sub-basin (Maidment 1996) as:  $T_{lag} = \frac{L^{0.8}(S+1)}{1900Y^{0.5}}$  (Lag time is calculated in hour),  $L$ =Longest flow path,  $Y$ =average watershed land slope,  $S = \frac{1000}{CN} - 10$ , maximum retention in watershed (inches),  $CN$ =curve number.

**Table 3** Soil texture and properties in each sub-basin

Sub-basin	Total area	Bulk density	Porosity	Field capacity	Texture class
W120	226,703,700	1.438, 1.328	0.457, 0.498	0.28, 0.24, 0.27	Loam, clay
W130	259,586,100	1.279, 1.439, 1.417	0.517, 1	0.43, 0.29, 0.28, 0.31	Clay, loam, clay loam
W140	245,180,700	1.404, 1.429, 1.466, 1.450, 1.412, 1.290	0.47, 0.51	0.39, 0.29, 0.15, 0.27	Clay, loam, sandy loam, loam, clay
W150	183,384,000	1.436, 1.411, 1.439, 1.429, 1.390	0.458, 0.507	0.29, 0.33, 0.28, 0.1, 0.32, 0.41	Loam, clay loam, loam, sand, clay
W160	337,167,000	1.438, 1.423, 1.457	0.517, 0.445, 0.502	0.43, 0.44, 0.28, 0.27, 0.3, 0.15, 0.39	Clay, loam, sandy-loam, clay
W170	120,717,900	1.438, 1.429, 1.260	0.457, 0.524	0.27, 0.29, 0.28, 0.30, 0.1, 0.43	Loam, sand, clay
W180	24,174,000	1.426, 1.435	0.462	0.29, 0.28	Loam
W190	3,252,600	1.458, 1.460	0.449	0.304, 0.15	Loam, sandy loam
W200	192,708,900	1.419, 1.439, 1.440	0.464, 0.456, 0.515	0.3, 0.29, 0.28, 0.32, 0.39, 0.31, 0.28	Loam, silty clay, silt loam, loam
W210	27,611,100	1.423, 1.438, 307, 1.445	0.462, 0.506	0.27, 0.28, 0.27, 0.32, 0.26, 0.31, 0.4, 0.41, 0.26	Loam, silty loam, clay, loam
W220	152,842,500	1.437, 1.423, 1.257	0.457, 0.568, 0.526	0.29, 0.28, 0.27, 0.43, 0.26, 0.3, 0.27	Loam, clay, silty clay

### 4.1.3 Modeling baseflow

As the recession method showed the best fit for observations (De Silva et al. 2014), this baseflow method was employed for both event-based and continuous simulations. The parameter recession constant describes the rate at which base flow recedes between storm events (Scharffenberg and Fleming 2006). The relevant parameters calibrated in event modeling were used in continuous modeling.

### 4.1.4 Routing model

The Muskingum method, developed by McCarthy (1938), was a simple mass storage approach for stream routing across a stream. The two essential parameters that travel through reach are the travel time ( $K$ ) of the flood wave through the routing reach and the dimensionless weight ( $X$ ) which corresponds to the attenuation of the flood wave. These values were obtained during calibration process. Here,  $X$  is a weighting factor which ranges from 0 to 0.5 (Scharffenberg and Fleming 2006).

## 4.2 Calibration and validation

Models are calibrated and validated by comparing the simulated with the observed stream flow for the evaluation of goodness of fit. The parameters were first calibrated using auto-calibration methods available in the HEC-HMS model. Fine-tuning of parameters was done using manual calibration (Merwade 2016). The validation process used the optimized parameters to simulate the other flood events.

Model performance efficiency criteria such as PEV, PEPF, NSE were used in this study to evaluate the goodness of fit during the calibration and validation periods. The ranking of the model performance is listed in Table 4 (Adib et al. 2010; Roy et al. 2013; Moriasi 2007; Singh et al. 2004).

The percentage error in peak flow:

$$PEPF = \frac{Q_{\text{opeak}} - Q_{\text{speak}}}{Q_{\text{opeak}}} \times 100 \tag{8}$$

The percentage error in volume:

$$PEV = \frac{\text{Vol}_o - \text{Vol}_s}{\text{Vol}_o} \times 100 \tag{9}$$

The percentage error in peak time of flood hydrograph (%):

**Table 4** Model performance ratings statistics

NSE	PEV (%)	PEPF (%)	PETP (%)	Performance ratings
0.75–1.00	< ± 10	< 15	< ± 10	Very good
0.65–0.75	± 10 to ± 15	15–30	± 10 to ± 15	good
0.50–0.65	± 15 to ± 25	30–40	± 15 to ± 30	satisfactory

$$\text{PETP} = \frac{T_{\text{pobs}} - T_{\text{psim}}}{T_{\text{pobs}}} \times 100 \quad (10)$$

$$t_{\text{peak error}} = \frac{T_{\text{pobs}} - T_{\text{psim}}}{T_{\text{pobs}}} \quad (11)$$

Nash–Sutcliffe efficiency:

$$\text{NSE} = 1 - \left[ \frac{\sum_{i=1}^n (Q_i^{\text{obs}} - Q_i^{\text{sim}})^2}{\sum_{i=1}^n (Q_i^{\text{obs}} - Q_{\text{mean}})^2} \right] \quad (12)$$

where  $Q^{\text{obs}}$  is observed flows,  $\text{m}^3/\text{s}$ ;  $Q^{\text{sim}}$  is simulated flows,  $\text{m}^3/\text{s}$ ;  $Q_{\text{avg}}$  is average observed flow,  $\text{m}^3/\text{s}$ ;  $\text{Vol}_o$  is observed volume, mm;  $\text{Vol}_s$  is simulated volume, mm;  $T_{\text{pobs}}$  is the observed peak time of flood hydrograph (hr);  $T_{\text{psim}}$  is the simulated peak time of flood hydrograph (hr);  $n$  is the number of points.

## 5 Results

### 5.1 Model calibration and validation

#### 5.1.1 Event-based simulations

The eight extreme rainfall events of wet period were used for the simulations. The flood events of 1973 August, 1976 July, 1977 June, 1978 July, 1982 July and 1987 July were used for calibration. The events of 1988 August and 1998 July were taken for validation.

The calibrated model parameters are listed in Tables 5 and 6. The observed and simulated streamflow hydrographs for calibration are shown in Fig. 4 and for validation in Fig. 5.

**Table 5** Calibrated model parameters of sub-basins

Sub-basin	CN	Lag time (min)	Recession constant
W120	37	361	0.59
W130	36	356	0.81
W140	44	105	0.54
W150	41	512	0.81
W160	38	155	0.81
W170	46	384	0.32
W180	80	380	0.53
W190	71	104	0.81
W200	40	208	0.44
W210	94	122	0.81
W220	64	109	0.59

**Table 6** Optimized model parameters of Reach

Reach	$K$ (hr)	$X$
R100	2.31	0.10
R20	1.21	0.10
R50	20.82	0.13
R70	11.45	0.45
R80	2.34	0.15

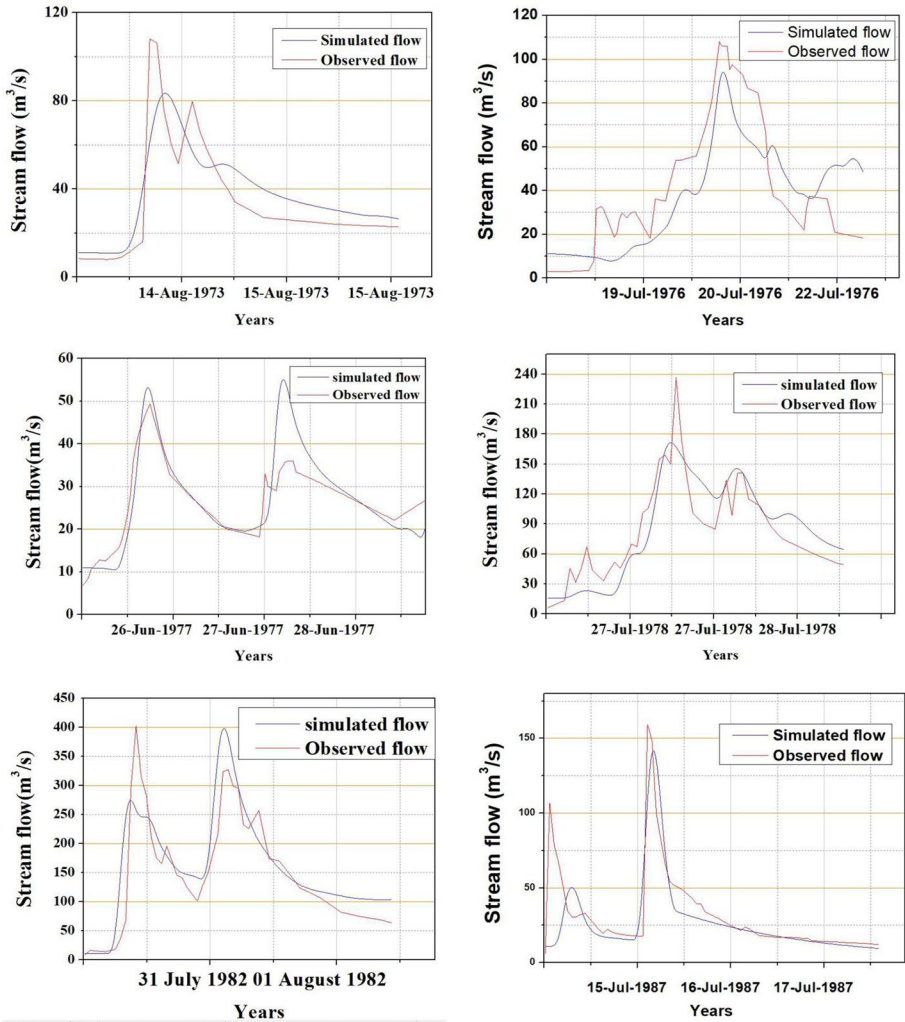


**Fig. 4** Simulated and observed hydrographs during calibration period

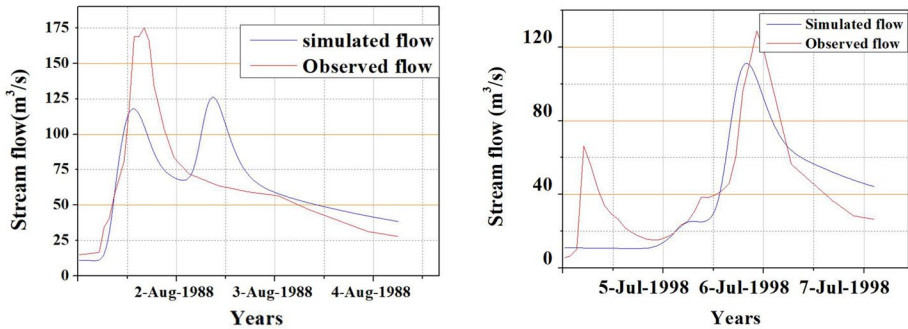


Fig. 5 Simulated and observed hydrographs during validation period

### 5.1.2 Continuous simulations

The hourly discharges in wet seasons of 1973, 1976, 1977, 1978, 1982 and 1988 were selected for calibration, and those in wet season of 1987 and 1998 were selected for validation. A continuous multi-year simulation was not performed because rainfall data and stream flow data of this basin are available for the wet period only.

The observed and simulated streamflow hydrographs of the calibration and validation period are shown in Figs. 6 and 7, respectively. For the peak values, the simulated and observed streamflow comparison indicates close match between them, and an acceptable match for streamflow distribution. The calibrated parameters are listed in Table 7. The parameters optimized during calibration were used as input parameters for validation of the model.

## 5.2 Model performance evaluation

For the event-based and continuous modeling, performance evaluation was conducted for each flood event during calibration and validation period. For the SCS-CN model, the values of NSE, PEV, PEPF during calibration range from 0.605 to 0.744, 3.1 to 13.58%, 11.10 to 27.72%, respectively, and for validation are 0.527 and 0.634, 4.35% and 5.01%, 13.66% and 27.88%, respectively. These values indicate good performance of the model. For the event-based modeling, the model has performed from satisfactory to very good range with all evaluation criteria. Similarly, for the SMA model the values of NSE, PEV, PEPF during calibration range from 0.434 to 0.604, 2.88 to 34.33%, -4.83 to 57.48%, respectively, and for the validation are 0.094 to 0.624, -19.52% to -12.55%, and 40.21% to 50.15%, respectively. According to the statistical evaluation of the SMA model, the results show satisfactory performance for both calibration and validation periods except for the periods 1977 and 1987, where NSE value is 0.434 and 0.094. Likewise, for the peak flow error (PEPF), it shows unsatisfactory results for periods 1973, 1978, 1987 and 1998. For PEV, the ranges of values indicate good model performance. This uncertainty in results of SMA model may be due to the lack of sufficient continuous observed data for long duration and topography. The performance evaluation values of calibration and validation for event-based model and continuous model are shown in Table 8.

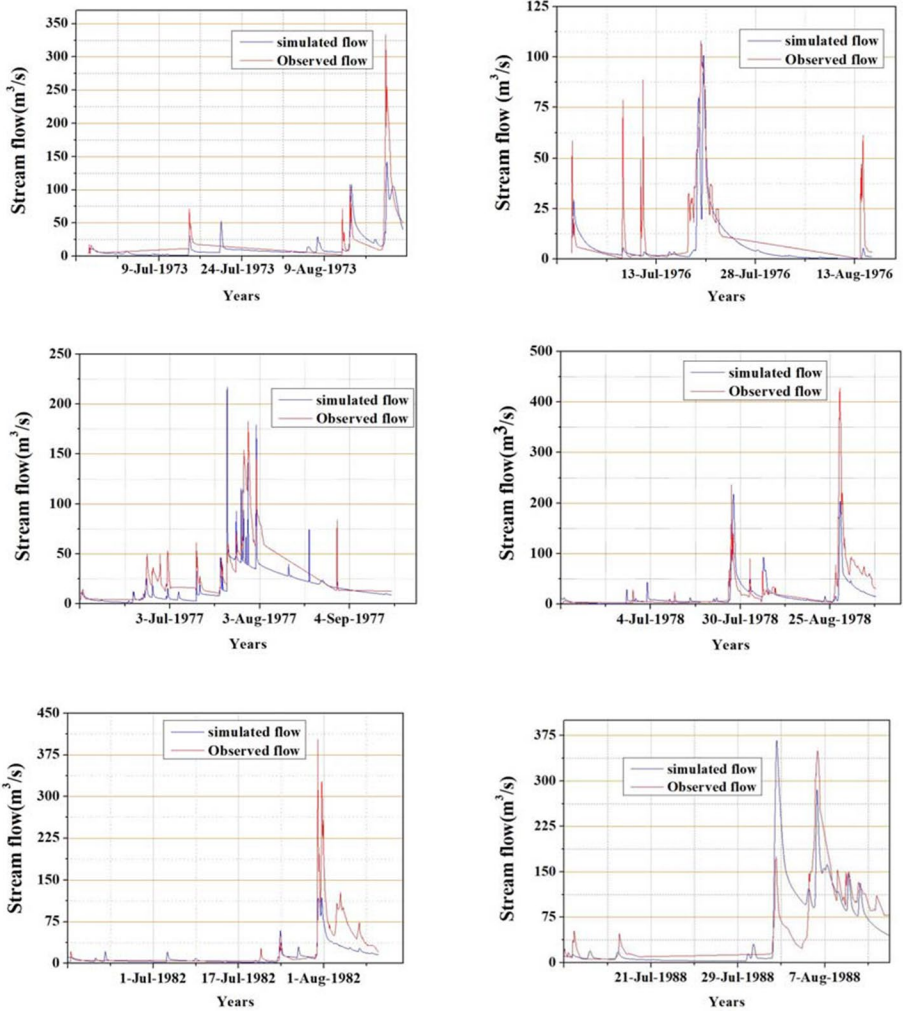


Fig. 6 Simulated and observed hydrographs during calibration period

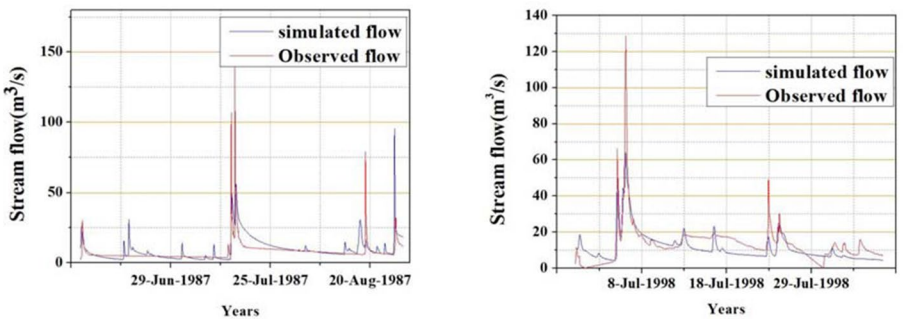


Fig. 7 Simulated and observed hydrographs during validation period

**Table 7** Calibrated parameters in continuous model

Sub-basin	Max canopy (mm)	Max surface (mm)	Soil (%)	Lag time (min)	Recession k	Max infiltrat (mm/hr)	Soil storage (mm)	Tension storage (mm)	Soil percol (mm/hr)	GW1 percol (mm/hr)	GW2 percol (mm/hr)
W120	12.73	15.62	9.42	195.41	0.75	9.91	51.87	33.35	14.95	9.93	9.84
W130	2.47	15.48	10.43	604.85	0.91	22.57	67.96	18.33	35.03	14.83	1.98
W140	13.02	2.51	13.09	1140.7	0.55	19.37	167.83	37.32	16.68	14.83	37.23
W150	2.14	0	7.91	378.38	0.97	16.39	249.65	86.28	16.68	14.83	11.56
W160	2.38	10.28	9.73	782	0.82	22.54	58.28	13.69	16.68	14.83	16.47
W170	6.37	0	8.03	958	0.16	21.14	253.99	23.59	16.95	14.83	11.98
W180	2.13	6.56	2.14	888.74	0.43	23.89	85.21	43.63	16.67	14.83	10.72
W190	1.86	0	1.53	103.9	0.01	4.167	46.6	21.62	16.68	14.83	11.03
W200	10.08	0.21	10.21	104.12	0.24	26.86	212.87	56.77	34.79	15.44	16.78
W210	2.92	0	1.95	266.28	0.95	10.17	85.86	58.07	35.87	14.83	2.17
W220	7.30	9.5	5.95	827.15	0.65	24.83	203.89	17.96	35.99	14.89	16.63



**Table 8** Performance evaluation of continuous model for the same time period as event model

Years	PEPF (%)	PEV (%)	NSE	$t_{peak}$ error
1973	0.27	−61.8	−0.99	1.8
1976	6.6	29.2	0.263	1.22
1977	70	76.22	−11.03	3.25
1978	1.6	−27.88	−1.84	0.76
1982	70.5	52.7	−0.234	2.15
1987	55.08	−13.12	0.065	1.34
1988	52.27	−168.74	−9.812	0.09
1998	50.15	10.37	0.525	0

### 5.3 SCS-CN-based and SMA-based model performance comparison

In this study, the simulated stream flows are compared with observed flows to find out which model (CN based or SMA based) simulates flood events better. Berthet et al. (2009) stated that an objective function, time to peak error, and a visual comparison of the observed and simulated hydrographs can serve as a basis for determining the better modeling. On the basis of the simulated hydrographs, it shows SMA-based model correctly simulates the general shape and magnitude of the hydrographs, but it could not specify the flow characteristics as SCS-CN-based model does. The SMA-based model simulates a fairly smooth hydrograph, while the SCS-CN-based model gives the similar shape and magnitude as the observed streamflow. This is observed in both calibration and validation. For the time to peak error ( $t_{peak}$ ), SMA exhibits greater error than SCS-CN-based model (Table 9). For the year 1973, SMA-based model shows 462% more error than SCS-CN-based model. Similarly, in 1976, 1977, 1978, and 1987, SMA-based model exhibits 100%, 31.27%, 16.6% and 22% more error, respectively. Only in 1988 and 1998, SCS-CN-based model exhibits 73% and 15% more error than SMA-based model. Therefore, SCS-CN-based model performs better than SMA-based model.

To further determine which model simulates flood events better, the same flood events were selected for the SMA model as the SCS CN model. Four performance criteria were evaluated (Table 10) for the SMA modeling results. It shows that NSE, PEV, PEPF and  $t_{peak}$  error values vary from −11.03 to 0.525, −61.80 to 76.22%, 0.27 to 70.52% and 0 to 3.25 (hr), respectively, while for SCS-CN model, NSE, PEV, PEPF

**Table 9** Time to peak error PETP (%)

Years	SCS-CN	SMA
1973	−37.50	−500.00
1976	−21.87	−121.87
1977	2.94	34.21
1978	5.26	−21.87
1982	84.37	84.37
1987	−6.57	28.94
1988	93.18	−20.00
1998	15.00	0.00

**Table 10** Performance evaluation for event-based and continuous simulation model

Years	Event-based simulation			Continuous simulation		
	PEPF (%)	PEV (%)	NSE	PEPF (%)	PEV (%)	NSE
1973	23.14	12.74	0.744	57.48	−19.14	0.608
1976	12.87	7.01	0.605	6.60	34.22	0.529
1977	11.56	8.14	0.644	−18.83	34.33	0.434
1978	27.72	3.12	0.741	49.01	23.50	0.542
1982	1.02	11.29	0.756	70.5	41.56	0.554
1988	27.88	4.35	0.527	−4.831	2.88	0.505
1987	11.10	13.58	0.616	40.21	−19.52	0.094
1998	13.66	5.01	0.634	50.15	−12.55	0.624

and  $t_{\text{peak}}$  error values range from 0.527 to 0.744, 3.1 to 13.58%, 11.10 to 27.88%, 0.03 to 0.93 (hr), respectively (Tables 8, 9). It can be concluded that SCS-CN model simulates flood events better than SMA model for the same time period.

## 6 Discussion

For rainfall-runoff modeling of the Zijinguan watershed, SCS-CN and SMA methods in HEC-HMS were used, respectively. The data used in SMA model required dense observation and high accuracy, which was not available in this research. Satellite data and standard data obtained from secondary sources were used (Azmat et al. 2017). With such data, the results were satisfactory for both event and continuous modeling. In the simulation, it was clearly seen that the simulated peak discharges coincided with the observed. The values of evaluation indicators NSE, PEPF, PEV ranged from satisfactory to very good for event-based modeling, and for continuous modeling the values ranged from acceptable to satisfactory. In continuous modeling, the years 1977 and 1987 showed very low Nash–Sutcliffe efficiencies just in acceptable range. In SMA model, evapotranspiration data have less effects on peak discharge because of its seasonal input in modeling.

Initial soil moisture used in this study was derived from satellite data. Soil saturation was used as initial condition to run the model. Increase of 20% initial soil saturation led to changes in peak flow ranging from −0.21 to 34.57%, and flood volume from −1.32 to 32.72%. Similarly, decrease of 20% initial soil saturation led to changes in peak flow ranging from −0.14 to −15.85%, and flood volume from −3.87 to 1.35%. It can be concluded that initial soil moisture has significant effects in modelled peak flow and flood volume. Therefore, the accuracy of the remote sensing soil moisture data should be guaranteed.

The results of event modeling showed that the model was able to reproduce peak discharge, peak time, and hydrographic recession curves accurately. From the results of continuous simulation, it can be assumed that if precipitation data, streamflow data, soil moisture and ground water data of the whole year are available, the calibrated SMA model can be used for long-term hourly runoff simulation, which will be further studied.

## 7 Conclusions

For the Zijinguan watershed, the event-based and continuous modeling of the HEC-HMS model has been successfully calibrated and validated. The applications of the two methods show the capability of HEC-HMS in simulating streamflow by combination of different soil, LULC and evapotranspiration data to improve the modeling ability. General criteria for evaluating the model were found to be satisfactory to very good during the calibration and validation period for event modeling, and for the continuous modeling the results were normally satisfactory. It can be concluded that SCS-CN-based model performs better than SMA-based model in the Zijinguan watershed. In this research, SCS-CN model needs less time and data than SMA model, and is more reliable.

**Acknowledgements** This work is supported by National Key R&D Program of China (No. 2018YFC0407902) and National Natural Science Foundation of China (No. 51779165). We would like to thank Hydrology and Water Resource Survey Bureau of Hebei Province for providing the hydrometeorological data.

**Funding** This work is supported by National Key R&D Program of China (No. 2018YFC0407902) and National Natural Science Foundation of China (No. 51779165).

## References

- Abouzar N, Hamid A (2014) Determination the curve number catchment by using GIS and remote sensing. *Int J Geol Environ Eng* 8:1–5
- Abushandi EH, Abushandi BJ (2011) Application of IHACRES rainfall-runoff model to the Wadi Dhuliel arid catchment, Jordan. *Water Res Manag* 27:2391–2409
- Abushandi EH, Merkel BJ (2011) Application of IHACRES rainfall-runoff model to the Wadi Dhuliel arid catchment, Jordan. *Water Res Manag* 27:2391–2409
- Adib A, Salarijazi M, Najafpour K (2010) Evaluation of synthetic outlet runoff assessment models. *J Appl Sci Environ* 14:13–18
- Agrawal A (2005) A data model with pre- and post-processor for HEC-HMS. Rep. of Graduate Studies, Texas A&M Univ., College Station
- Ahbari A, Stour A, Agoumi SN (2018) Estimation of initial values of the HMS model parameters: application to the basin of Bin El Ouidane. *J Mater Envir Sci* 9:305–317
- Arekhi S (2012) Runoff modelling by HEC-HMS Model (Case-Study: Kan Watershed, Iran). *Inter J Agri Crop Sci* 23:1807–1811
- Azmat M, Choi M, Kim TW et al (2016) Hydrological modeling to simulate streamflow under changing climate in a scarcely gauged cryosphere catchment. *Environ Earth Sci* 75:1–16
- Azmat M, Qamar MU, Ahmed S, Hussain E, Umair M (2017) Application of HEC-HMS for the event and continuous simulation in high altitude scarcely-gauged catchment under changing climate. *Eur Water* 57:77–84
- Baumbach T, Burckhard SR, Kant JM (2015) Watershed Modeling Using Arc Hydro Tools. Geo HMS, and HEC-HMS. Civil and Environmental Engineering Faculty Publications
- Bediet PB, Holder A, Benavides JA et al (2003) Radar-based flood warning system applied to Tropical Storm Allison. *J Hydrol* 8:308–318
- Bennett T (1998) Development and application of a continuous soil moisture accounting algorithm for the hydrologic engineering center hydrologic modeling system (HEC-HMS). University of California, Davis, California
- Berthet L, Andréassian V, Perrin C et al (2009) How crucial is it to account for the antecedent moisture conditions in flood forecasting? Comparison of event-based and continuous approaches on 178 catchments. *Hydrol Earth Syst Sci* 13:819–831
- Bhuiyan AKM, McNairn H, Powers J et al (2017) Application of HEC-HMS in a cold region watershed and use of RADARSAT-2 soil moisture in initializing the model. *J Hydrol* 9:1–19

- Brocca L, Melone F, Moramarco T et al (2010) Improving runoff prediction through the assimilation of the ASCAT soil moisture product. *Hydrol Earth Syst Sci* 14:1881–1893
- Chow VT, Maidment DR, Mays LW (1988) *Applied Hydrology*. McGraw-Hill, New York
- Chu XF, Alan S (2009) Event and continuous hydrologic modeling with HEC–HMS. *J Irrig Drain Eng* 135:119–124
- Cunderlik MJ (2003). Hydrologic model selection for the CFCAS project: assessment of water resources risk and vulnerability to changing climatic conditions. The University of Western Ontario
- Davie T (2002). *Fundamentals of Hydrology*. 1st edn., Routledge, London and New York
- Davis CA, Singh J, Knapp HV, Demissi M (2004) Hydrologic modeling of the Iroquois River watershed using HSPF and SWAT. Champaign, Ill.: Illinois State Water Survey
- De Silva MMTG, Weerakoon SB, Herath S (2014) Modeling of event and continuous flow hydrographs with HEC–HMS: case study in the Kelani River basin, Sri Lanka. *J Hydrol Eng* 19:800–806
- Feldman AD (2000) Hydrologic modeling system HEC-HMS, Technical reference manual. U.S. Army Corps of Engineers, Hydrologic Engineering Center HEC: Davis, USA
- Fleming M, Neary V (2004) Continuous hydrologic modeling study with the hydrologic modeling system. *J Hydrol Eng* 9:175–183
- Gandini ML, Usunoff EJ (2004) SCS curve number estimation using remote sensing NDVI in a GIS environment. *J Environ Hydrol* 12:1–16
- Hawkins RH, Ward TJ, Woodward DE (2009) *Curve number hydrology: state of the practice*. Environmental and Water Resources Institute, VA, USA
- Holberg J (2014) Tutorial on using HEC-GeoHMS to develop soil moisture accounting method inputs for HEC-HMS. Purdue University, West Lafayette
- Jajarmizadeh M, Harun S, Salarpour M (2012) A review on theoretical consideration and types of models in hydrology. *J Environ Sci Technol* 5(5):249–261
- Kaczmarek Z (1976) Applications of stochastic models in hydrology. *Hydrol Sci J* 21(1):5–11
- Li SY, Qi RZ, Jia WW (2008) Calibration of the conceptual rainfall-runoff model's parameters. In: *Proceeding of 16th IAHR-APD congress and 3rd symposium of IAHR-ISHS*, Tsinghua University Press, Beijing, pp 55–59
- Li Y, Grimaldi S, Walker JP, Pauwels VRN (2016) Application of remote sensing data to constrain operational rainfall-driven flood forecasting: a review. *Remote Sens* 8:1–29
- Li J, Zhou K, Zhang T, Ma Q, Feng P (2019) Analysis of flood peak scaling in mesoscale non-nested basin. *Water Suppl* 20(2):416–427
- Madsen H (2000) Automatic calibration of a conceptual rainfall–runoff model using multiple objectives. *J Hydrol* 4:276–288
- Maidment D (1996) *A Study of hydrologic simulation models, rainfall/runoff simulation*, Term Paper- 394K Surface Water Hydrology.
- McCarthy GT (1938) *The unit hydrograph and flood routing*. North Atlantic Division, US Army, Corps of Engineers
- McCuen RH (1998) *Hydrologic Analysis and Design*, 2nd edn. Prentice Hall, Upper Saddle River, p 814
- Meenu R, Rehana S, Mujumdar PP (2013) Assessment of hydrologic impacts of climate change in Tungabhadra river basin, India with HEC-HMS and SDSM. *Hydrol Process* 27:1572–1589
- Merwade V. 2016. HEC-HMS Lab 9: Model Calibration, Purdue University.
- Milad J, Sobri H, Mohsen S (2012) A review on theoretical consideration and types of models in Hydrology. *J Environ Sci Technol* 5:249–261
- Moriasi DN, Arnold JG, Liew MWV, Bingner RL, Harmel RD, Veith TL (2007) Model evaluation guidelines for systematic quantification of accuracy in watershed simulations. *T ASABE* 50:885–900
- Oleyiblo JO, Li Z (2010) Application of HEC-HMS for flood forecasting in Misai and Wan'an catchments in China. *Water Sci Eng* 3:14–22
- Ouédraogo WA, Raude JM, Gathenya JM (2018) Continuous modeling of the Mkurumudzi River catchment in Kenya using the HEC-HMS conceptual model: calibration, validation, model performance evaluation and sensitivity analysis. *J Hydrol* 44:1–18
- Pandey, A. and A. K. Sahu, 2007. *Generation of curve number using remote sensing and Geographic Information System*.
- Roy D, Begam S, Ghosh S et al (2013) Calibration and validation of HEC-HMS model for a river basin in eastern India. *J Eng Appl Sci* 8:40–56
- Samarasinghe SMJS, Nandalal HK, Welivitiya DP et al (2010) Application of remote sensing and GIS for flood risk analysis: a case study at Kalu-Ganga river, Sri Lanka. *Remote Sens Spat Inf Sci* 38:110–115
- Scharffenberg W A, Fleming M J. 2006. *Hydrologic modeling system HEC–HMS user's manual*. U.S. Army Corps of Engineers, Institute for Water Resources, Hydrologic Engineering Center

- Singh J, Knapp HV, Demissi M (2004) Hydrologic modeling of the Iroquois River watershed using HSPF and SWAT. Illinois State Water Survey, Champaign, Ill
- Singh WR, Jain MK (2015) Continuous hydrological modeling using soil moisture accounting algorithm in Vamsadhara River basin, India. *J Water Resour and Hydraul Eng* 4:398–408
- Soil Conservation Service, United States Department of Agriculture (SCS-USDA) (1986) *Urban Hydrology for Small Watersheds*. U. S. Government Printing Office, Washington D C
- Stisen S, Jensen K (2008) A remote sensing driven distributed hydrological model of the Senegal river basin. *J Hydrol* 354:131–148
- Sutanudjaja EH, van Beek LPH, de Jong SM et al (2013) Calibrating a large-extent high-resolution coupled ground-water-land surface model using soil moisture and discharge data. *Water Resour Res* 50:687–705
- Tassew BG, Belete MA, Miegel K (2019) Application of HEC-HMS Model for Flow Simulation in the Lake Tana Basin: The Case of Gilgel Abay Catchment, Upper Blue Nile Basin, Ethiopia. *J Hydrol* 6(1):1–17
- Todini E (1996) The ARNO rainfall–runoff model. *J Hydrol* 175:339–382
- Tramblay Y, Bouaicha R, Brocca L et al (2012) Estimation of antecedent wetness conditions for flood modelling in northern Morocco. *Hydrol Earth Sys Sci* 16:4375–4386
- United States Army Corps of Engineers, Hydrologic Engineering Center (USACE HEC-GeoHMS) (2006) *Geospatial Hydrologic Modeling Extension. User's Manual*, Davis, California
- Urban Hydrology for Small Watershed, United States Department of Agriculture, Technical Release 55. US Army Corps of Engineers (2000) Hydrologic Engineering Center, HEC. *Hydrologic Modeling System, Users' Manual*.
- USACE (2015) *Hydrologic Modeling System, HEC-HMS. Quick Start Guide*; US Army Corps of Engineers Institute for Water Resources Hydrologic Engineering Center: Davis, CA, USA
- Yener MK, Orman AÜ (2008) Modeling studies with HEC-HMS and runoff scenarios in Yuvacik Basin, Turkiye. Middle East Technical University, Türkiye
- Yu Z, Schwartz FW (1998) Application of an integrated basin-scale hydrologic model to simulate surface-water and groundwater interactions. *J Am Water Resour Assoc* 34:1–17
- Zdzislaw K (1976) Applications of stochastics models in Hydrology. *Hydrol Sci J* 21(1):5–11
- Zhan X, Huang ML (2004) ArcCN-Runoff: an ArcGIS tool for generating curve number and runoff maps. *Environ Model Softw* 19:875–879

**Publisher's Note** Springer Nature remains neutral with regard to jurisdictional claims in published maps and institutional affiliations.